



Load frequency control of autonomous power system using adaptive fuzzy based PID controller optimized on improved sine cosine algorithm

K. S. Rajesh¹ · S. S. Dash¹

Received: 5 December 2017 / Accepted: 3 May 2018 / Published online: 18 May 2018
© Springer-Verlag GmbH Germany, part of Springer Nature 2018

Abstract

An autonomous power generation system contains numerous autonomous generation units like diesel energy generator, solar photovoltaic units, wind turbine generator, fuel cells along with energy storing units such as the flywheel energy storage system and battery energy storage system. These renewable sources are typically varying in nature. Therefore, the system components either run at lower/higher power output or may turned on/off at different instant of their operation. Due to the above mentioned uncertainties, the conventional controllers are not able to provide desired performance under varied operating conditions. Owing to this challenge, this paper proposes an adaptive fuzzy logic PID controller (AFPID) optimized by improved sine cosine algorithm (ISCA) for the load frequency control (LFC) of an autonomous power generation system. Proposed ISCA algorithm is evaluated using standard test functions and compared with original sine cosine algorithm (SCA) to authenticate the competence of algorithm. It is found from the statistical results that the proposed ISCA algorithm outperform original SCA, Hybrid Improved Firefly-Pattern Search, gravitational search, and grey wolf optimization algorithms. The proposed AFPID controller optimized by ISCA is used for the load frequency control of the autonomous power generating system. The results show that the ISCA tuned AFPID controller has superior performance over conventional PID controller. The proposed AFPID controller is again examined by the sensitivity analysis by introducing different hybrid power system parameters and the robustness of the control approach with the dynamic change of power system parameters is evaluated. Finally, the stability of the proposed control system is tested using Eigen value analysis.

Keywords Autonomous power generation system · Load frequency control (LFC) · Sine cosine algorithm (SCA) · Adaptive fuzzy logic PID controller (AFPID)

1 Introduction

The increasing power demand, rising costs of electricity transmission and distribution, deregulation of the energy markets, depletion of fossil fuels are making a significant entrance of renewable energy sources into the energy sector (Pan 2016; Ray et al. 2010, 2011; Lee and Wang 2008). The centralized power generation, transmission and distribution are now shifting to decentralized one (Pan 2016). In this framework, a new power system model called autonomous power generating system (APGS) has been evolved. It is

a combination of distributed energy resources (DERs) like diesel energy generator (DEG), fuel cell (FC) with renewable energy sources like solar photovoltaic (PV) units, wind turbine generators (WTG), batteries, flywheels etc. and cluster of loads (Pan 2016; Ray et al. 2010). The APGS aspires to provide high quality as well as reliable service to its consumer and this is determined by the type and action of the controller implemented in the power system.

Due to the gradual progression in the innovation, reduced price of the components and scarcity of fossil fuels, wind energy is taking a lead renewable energy choice in APGS. Similarly photovoltaic energy is also growing very fast to meet the increasing power demand due to improvement in the semiconductor technology. But, both the energy sources are highly unstable in nature due to unpredictable environmental conditions. The chaotic characteristic of the load and the sustainable energy generations i.e. wind and solar

✉ K. S. Rajesh
rajeshks.srm@gmail.com

¹ Department of Electrical Engineering, SRM University, Chennai, India

sources introduce fluctuations in the system frequency (Pan 2016). Energy storing elements like ultra capacitor (UC), flywheel energy storage system (FESS), and battery energy storage system (BESS) are coupled to the system to mitigate the unbalance due to generation and load mismatch. These energy storing devices store the surplus power for a small interval of period from the renewable energy sources and later deliver the power to the grid when the demand load is more (Pan 2016, 2015). A proper control strategy is required for coordinating these actions accurately (Pan 2016). This calls for the concept of load frequency control (LFC) for damping the frequency oscillation in the framework of hybrid power system.

The prime responsibility of the LFC in the system is to make a power balance in such a way that the system dynamic performance is reasonably maintained and the system frequency deviation always remains within prespecified limits. An appropriate LFC results in fuel saving thus making the system more energy efficient and decreases the requirement of more protective arrangement there by reducing the cost of maintenance (Khooban et al. 2017). In order to enhance the performance of the LFC, several control approaches like the conventional PID controller (Ray 2011; Nandar 2013), robust H_∞ controller (Singh et al. 2013; Mohanty et al. 2014; Bevrani et al. 2015; Pandey et al. 2014), Fractional order controller (Pan 2016; Pan and Das 2016) have been used in similar kind of system design.

To preserve desirable performance and stability, either centralized controller (Pan and Das 2015) or decentralized controller (Ray et al. 2011; Senjyu et al. 2005) is mostly used. Our work has focused on centralized controller scheme. In this method, the system parameters and the local loads of the hybrid power system are controlled by a centralized control unit rather than multiple decentralized controllers. This makes the overall system design simple as well as reduces cost and wiring (Pan and Das 2016).

Under frequency load shedding (ULFS) schemes are devised to maintain the load-generation balance of the power system by shedding adequate loads to match the generation. Following an under frequency event, UFLS scheme is the last resort to arrest declining frequency and to preserve the security of both generation and transmission systems. As the conventional UFLS schemes are more rigid, several algorithms have been proposed to improve its adaptability. A three stage centralized adaptive load shedding is proposed by Aminifar and Shekari (2018). To meet the unintentional islanding in microgrid, an adaptive optimization based under frequency load shedding is proposed by Amin et al. (2018). A synchrophasors based two-unit wide-area adaptive load shedding scheme is proposed by Tohit et al. (2016). A strategy based on frequency information, rate of change of frequency, customers' willingness to pay, and loads histories,

to shed an optimal number of loads in the island to stabilize the frequency is presented by Pukar et al. (2010).

Conventional PI based controller was adopted by some of the researcher for load frequency control on similar kind of system (Ray et al. 2011; Nandar 2013). Before the introduction of fractional calculus based PID controller, robust H_∞ controller approach is also used by (Lee and Wang 2008; Mohanty et al. 2014; Bevrani et al. 2015; Pandey et al. 2014; Vachirasricirikul and Ngamroo 2012) for LFC problem. In recent years fractional calculus based control system design has made it in various power system applications like two area load frequency control (Pan and Das 2016; Sudha and Santhi 2011), microgrid LFC (Pan 2015), smart grid LFC by V2G (vehicle to grid) power control method (Vachirasricirikul and Ngamroo 2014) etc. Few papers addressed fuzzy logic techniques for optimal tuning of the standard PID controller (Bevrani et al. 2012; Savran and Kahraman 2014; Li et al. 2008) and FOPID controller (Pan 2016) for solving LFC problem. It is observed that, adaptive control makes the system under control less affected by the unmodeled process dynamics and variation in system parameter. Therefore, in the proposed control strategy, an adaptive fuzzy based PID controller is taken into consideration for LFC in the proposed hybrid power system.

Controlling APGS with various uncertain system parameters are mostly optimization based (Pan 2015; Rajesh et al. 2017a). Various artificial intelligence and hybrid optimization algorithms are validated in so many papers (Pan and Das 2016; Pan 2016; Khooban et al. 2017; Nandar 2013; Pandey et al. 2014; Bevrani et al. 2012; Rajesh et al. 2017a) to find the controller gains iteratively in order to enhance the system transient response, to deal with the practical issues as well as to ensure the robustness and stability of the system.

Sine cosine algorithm (SCA) is a recently proposed optimization technique which is based on the well known sine and cosine functions in which several random and adaptive variables are integrated for exploration and exploitation capability in the search space (Seyedali 2016). The superiority of SCA algorithm over particle swarm optimization (PSO), genetic algorithm (GA), bat algorithm (BA), flower pollination algorithm (FPA), firefly algorithm (FA), and gravitational search algorithm (GSA) has been reported in literature (Seyedali 2016). However, in original SCA algorithm the range of sine and cosine in the algorithm is changed linearly to maintain balance between exploration and exploitation stages. Since the position of the optimal design in the search space is not known a priori, this process of update may result in being stuck in local optima. Therefore, in the present paper an improved SCA (ISCA) is proposed where correction factors are introduced at various stages of the algorithm to get improved results. Proposed ISCA algorithm is first tested using some bench mark test functions and compared with original SCA to authenticate

the competence of the algorithm. The performance of proposed ISCA is also compared with Hybrid Improved Firefly-Pattern Search (hIFA-PS) Algorithm, gravitational search algorithm (GSA) and Grey Wolf Algorithm to illustrate the advantage of ISCA.

2 Sine cosine algorithm (SCA)

Sine cosine algorithm is a recently new developed optimization technique whose algorithm is based on sine and cosine mathematical functions (Seyedali 2016). The global optimal is obtained after several iteration steps with large number of random solutions. Optimization of this algorithm undergoes into two phases. In the exploration phase a promising region is formed by an optimization algorithm with the random solutions in the solution set at high rate while in the exploitation phase, the change of random solutions and random variation is slow and global optima is obtained. The mathematical modeling of sin and cosine algorithm is shown by the updating positions of solution for both phases is represented by

$$X_j^{t+1} = X_j^t + r_1 \times \sin(r_2) \times |r_3 P_j^t - X_j^t| \quad r_4 < 0.5 \quad (1)$$

$$X_j^{t+1} = X_j^t + r_1 \times \cos(r_2) \times |r_3 P_j^t - X_j^t| \quad r_4 \geq 0.5 \quad (2)$$

where X_j^{t+1} updating position of next solution in j th dimension at t -th iteration, X_j^t position of current solution, P_j^t is the target position in j th dimension, $r_1/r_2/r_3/r_4$ are the main parameters of SCA and are random numbers. The random number r_1 implies the next position's (movement) region, which could be inside or outside the solution space, r_2 leads the movement of position for a solution is towards or outwards the target destination. The number r_3 is the random weight supports to the destination position P_j^t emphasizing

the distance if $r_3 > 1$ and not emphasizing for $r_3 < 1$. The random number r_4 selects the sine and cosine components depending on the number.

The update position inside and outside can be extended by changing the range $(-2, 2)$ of sine and cosine functions and the random location inside and outside the region is possible for r_2 in $(0, 2\pi)$ as reported in (Seyedali 2016). To obtain the promising region and global optimum in search space, the exploration and exploitation must be balanced by the sine and cosine algorithm which is done by changing r_1 in the Eqs. (1) and (2) as

$$r_1 = a - t \left(\frac{a}{T} \right) \quad (3)$$

where, $a =$ constant (taken as 2 in the original SCA algorithm), $t =$ current iteration and $T =$ maximum number of iteration.

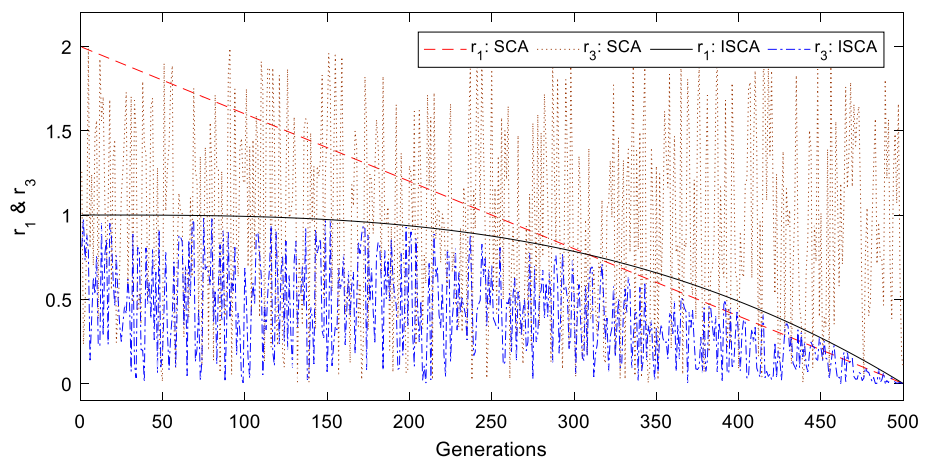
3 Improved SCA algorithm

For any meta-heuristic algorithm, a good balance between exploitation and exploration during search process should be maintained to achieve good performance. In improved SCA (ISCA) technique, to maintain a better balance between exploration and exploitation stages of the algorithm the parameter r_1 in the Eq. (3) is varied as Eq. (4):

$$r_1 = 1 - t^{31} \left(\frac{1}{T^3} \right) \quad (4)$$

In addition, the r_3 in proposed ISCA algorithm is made a dependent on random number as well as parameter r_1 and gradually decreases with generations. The variation of r_1 and r_3 with number of generation is shown in Fig. 1. Therefore both r_1 and r_3 are varied in an adaptive manner (gradually in the initial stages of generations and rapidly towards the

Fig. 1 Variation of parameters r_1 and r_3 during generations in original and proposed ISCA algorithms



later stages of generation) to improve the performance of the algorithm.

4 Performance investigation of ISCA algorithm

The performance analysis of proposed ISCA algorithm was carried out by fitting to some standard benchmark functions. The details about these functions, their dimension, boundary of the search spaces and optimum values are available in literature (Seyedali et al. 2014). There are 13 functions, out of which functions f_1 to f_7 are unimodal functions. Unimodal functions are specifically taken for verifying the exploitation property of the algorithm. Functions f_8 to f_{13} are multimodal function with more no. of local optima. This no. increases exponentially with the increase in dimensions. These functions are very challenging test beds for metaheuristic algorithms as exploration and exploitation can be simultaneously tested by these functions. As suggested in the original SCA algorithm, the ISCA algorithm was executed for 30 independent runs with randomly generated population for each benchmark functions with a population size of 30 and iteration of 500. The statistical results like average and standard deviation are gathered for original SCA and proposed ISCA for various dimension of functions f_1 to f_7 are shown in Table 1. A two-sided Wilcoxon rank sum test (Demsar 2006) is employed to assess the statistical significance of the observed differences between ISCA and SCA algorithms. At the 5% significance level, the tested hypothesis (H0) was that the compared results are independent ones from identical continuous distributions. As stated in Table 1, a “-” sign identifies the case where SCA shows an inferior to that of ISCA, and a “+” sign signifies when it exhibits superior performance. In such cases H0 is rejected. The cases when

the performance difference is not statistically significant, are marked with a “=” sign. Careful examination of the comparative results given in Table 1 indicates that the proposed ISCA algorithm outperforms the original SCA in a statistically significant manner. The results of proposed ISCA are compared with some recent techniques like PSO, GSA, and GWO (Seyedali et al. 2014). The mean and the standard deviation for 30 independent runs of all of the contestant algorithms on the unimodal benchmark problems for $D=30$ are given in Table 2. It is clear from Table 2 that proposed ISCA algorithm outperforms in 5 out of 7 functions and compares well in other 2 functions compared to the contestant algorithms. Similar comparative results for multimodal functions are shown in Tables 3 and 4. It is clear from Tables 3 and 4 that significantly better results are obtained with proposed ISCA technique compared to other techniques in this case also. This validates that ISCA makes a sound equilibrium between exploration and exploitation stages of algorithm.

5 Engineering application OF ISCA

The proposed ISCA technique is also applied to a real world problem of tuning the adaptive fuzzy logic controller for frequency control of autonomous power generation system. The block diagram of the proposed autonomous power generating system (APGS) using different generations and energy storage is presented in Fig. 2. Table 5 reports the parameter values of each component. The generation subsystem includes one PV, one DEG, two FCs and three WTGs. The storage system includes one BESS and one FESS connected to the load side. Moreover, appropriate rate constraint nonlinearities are considered

Table 1 Mean and standard deviation of the objective function values for functions f1–f9 averaged over 30 runs for unimodal test functions of various dimension

f	5D		10D		20D		30D	
	ISCA	SCA	ISCA	SCA	ISCA	SCA	ISCA	SCA
f1	0.246 E – 86 (0.1109E – 85)	0.097E – 29 (0.4312E – 29) +	0.443E – 57 0.2087E – 56	0.1428E – 9 0.7418E – 9 +	0.2157E – 37 (0.7131E – 37)	0.0227 (0.0780) +	0.696E – 29 (0.2099E – 28)	21.0038 (69.5623) +
f2	0.429E – 45 (0.2245E – 45)	0.794E – 18 (0.4331E – 18) +	0.3239E – 31 (0.7448E – 31)	0.941E – 9 0.1744E – 8 +	0.1592E – 21 (0.3882E – 21)	0.2471E – 3 (0.3511E – 3) +	0.0837E – 17 (0.1176E – 17)	0.0178 (0.0215) +
f3	0.448E – 77 (0.2448E – 76)	0.391E – 18 (0.1487E – 17) +	0.1775E – 48 (0.9026E – 48)	0.0121 0.0592 +	0.0844E – 28 (0.4417E – 28)	1.0638E3 (1.7568E3) +	0.575E – 22 (0.1963E – 21)	8.0222E3 (5.8196E3) +
f4	0.725E – 41 (0.3672E – 41)	0.578E – 12 (0.2453E – 12) +	0.456E – 27 (0.1530E – 26)	0.0017 (0.0043) +	0.3698E – 17 (0.6335E – 17)	7.5347 (5.1885) +	0.0725E – 12 (0.1098E – 12)	34.5259 (12.0554) +
f5	2.8273 (0.2692)	3.3701 (7.1625) =	7.9476 (0.2392)	37.6948 (166.3143) +	18.1239 (0.3220)	61.4415 (149.3944) +	28.3872 (0.3486)	0.7184E5 (1.7850E5) –
f6	0.0628 (0.0259)	0.0272 (0.0431) =	0.8523 (0.1178)	0.4476 (0.1494) =	3.0707 (0.1801)	2.5664 (0.3525) =	5.3957 (0.2006)	18.8163 (26.9175) +
f7	0.8221E – 4 (0.6349E – 4)	0.6435E – 3 (0.6715E – 3) =	0.1348E – 3 (0.1113E – 3)	0.0022 (0.0016) =	0.1503E – 3 (0.1475)	0.0194 (0.0185) +	0.1964 (0.1409)	0.1218 (0.0995) =

Table 2 Comparison of proposed ISCA with other techniques for unimodal benchmark test functions of 30D

f	ISCA		hIFA-PS		GSA		GWO	
	Avg.	Std. Dev	Avg.	Std. Dev	Avg.	Std. Dev	Avg.	Std. Dev
f1	0.696E-29	0.2099E-28	1.36E-20	2.02E-27	2.53E-16	9.67E-17	6.59E-28	6.34E-05
f2	0.0837E-17	0.1176E-17	4.21E-16	0.04E-15	0.055655	0.194074	7.18E-17	0.029014
f3	0.575E-22	0.1963E-21	0.71E-20	22.1E-18	896.5347	318.9559	3.29E-06	79.1498E-6
f4	0.0725E-12	0.1098E-12	1.08E-10	0.37E-10	7.35487	1.741452	5.61E-07	1.315088
f5	28.3872	0.3486	36.71832	60.1E-2	67.54309	62.22534	26.81258	69.9049
f6	5.3957	0.2006	0.000102	8.28E-05	2.5E-16	1.74E-16	0.816579	0.00012
f7	0.1964	0.1409	0.122854	0.044957	0.089441	0.04339	0.002213	0.10028

Table 3 Mean and standard deviation of the objective function values for functions f8–f13 averaged over 30 runs for multimodal test functions of various dimension

f	5D		10D		20D		30D	
	ISCA	SCA	ISCA	SCA	ISCA	SCA	ISCA	SCA
f8	-1.2528E3 (0.1634E3)	-1.5708E3 (0.1299E3)=	-1.6628E3 (0.2130E3)	0.0853E3 (0.0431E3)=	-2.1953E3 (0.2223E3)	-2.9880E3 (0.1622E3) =	-2.7698E3 (0.3730E3)	-3.7748E3 (0.2835E3)=
f9	0 (0)	0.0474E-14 (0.2595e-14) +	0 (0)	0.3050 (1.0955) +	0 (0)	12.3490 (17.1511) +	0 (0)	32.1439 (28.5467) +
f10	0.8882E-15 0	0.3020E-14 (0.2397E-14) =	0.8882E-15 0	3.4677E-4 (0.0018) +	0.8882E-15 0	5.7270 (8.2480) +	0.1007E-14 (0.0649E-14)	32.1439 (28.5467) +
f11	0 (0)	0.0187 (0.0561) +	0 (0)	0.1314 (0.2130) +	0 (0)	0.2511 (0.2465) +	0 (0)	1.0232 (0.3781) +
f12	0.0518 (0.0220)	0.0128 (0.0129) =	0.2274 (0.0599)	0.0912 (0.0363) =	0.5215 (0.0660)	0.8943 (0.9310) =	0.6796 (0.0767)	2.6329E4 (8.6000E4) +
f13	0.0853 (0.0431)	0.0332 (0.0307) =	0.5009 (0.0787)	0.3560 (0.0755) =	1.5640 (0.0732)	3.0416 (4.7619) =	0.6836 (0.0376)	1.2809E4 (4.9391E4) +

Table 4 Comparison of proposed ISCA with other techniques for unimodal benchmark test functions of 30D

f	ISCA		hIFA-PS		GSA		GWO	
	Avg.	Std. Dev	Avg.	Std. Dev	Avg.	Std. Dev	Avg.	Std. Dev
f8	-2.7698E3	0.3730E3	-4.29E2	1.152	-2821.07	493.0375	-6123.1	-4087.44
f9	0	0	6.70423	1.62938	25.96841	7.470068	0.310521	47.35612
f10	0.1007E-14	0.0649E-14	0.27E-12	0.509E-10	0.062087	0.23628	1.06E-13	0.07783E-13
f11	0	0	0.000925	0.007724	27.70154	5.040343	0.004485	0.006659
f12	0.6796	0.0767	0.006917	0.026301	1.799617	0.95114	0.053438	0.020734
f13	0.6836	0.0376	0.7429	1.814	-2821.07	493.0375	-6123.1	-4087.44

such $|P_{FESS}^*| < 0.9$, $|P_{BESS}^*| < 0.2$, $|P_{DEG}^*| < 0.01$. These rate constraint nonlinearities incorporate various electromechanical constraints that these devices exhibit.

5.1 Modelling of different generating systems

The PV, DEG, FC and WTG are represented by their first order transfer functions (5)–(8) with their corresponding gains and

Fig. 2 Block diagram representation of the autonomous power generating system considered in the study

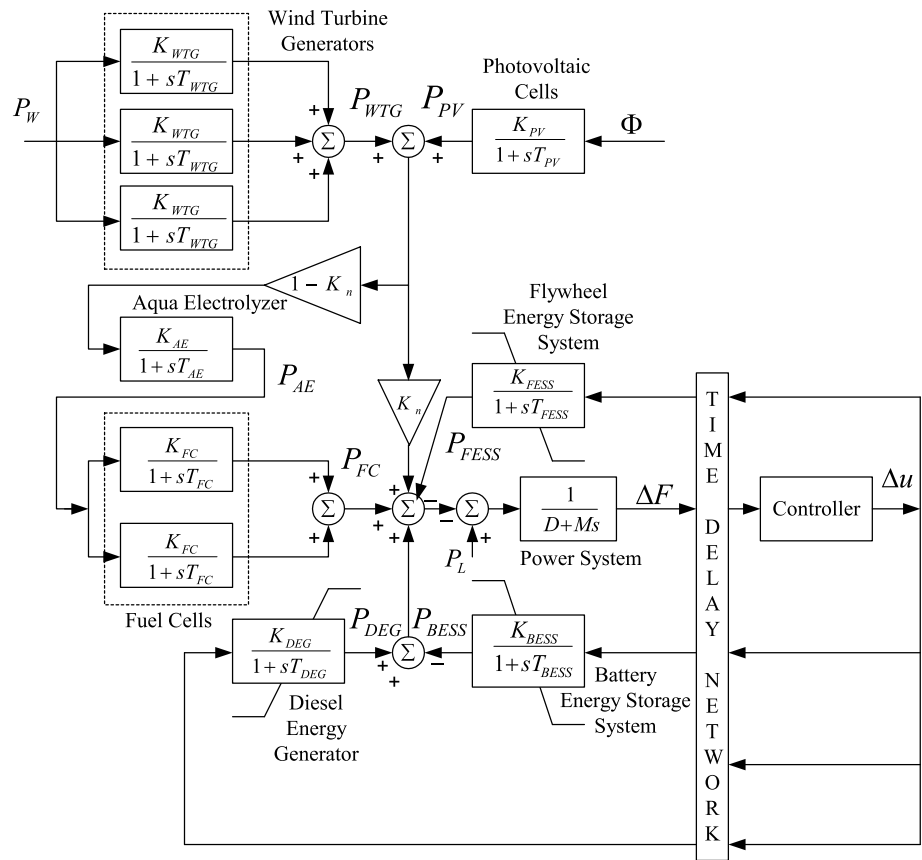


Table 5 Parameters of autonomous power generating system

Components	Gain	Time constant
Solar photovoltaic (PV)	$K_{PV} = 1$	$T_{PV} = 1.8$
Wind turbine generator (WTG)	$K_{WTG} = 1$	$T_{WTG} = 1.5$
Aqua electrolyzer (AE)	$K_{AE} = 0.02$	$T_A = 0.5$
Fuel cell (FC)	$K_{FC} = 0.01$	$T_{FC} = 4$
Diesel energy generator (DEG)	$K_{DEG} = 0.003$	$T_{DEG} = 2$
Battery energy storage system (BESS)	$K_{BESS} = -0.03$	$T_{BESS} = 0.1$
Flywheel energy storage system (FESS)	$K_{FESS} = -0.01$	$T_{FESS} = 0.1$

time constants reported in Table 5 (Pan and Das 2016; Lee and Wang 2008; Ray et al. 2011). The parameter k represents the no. of units considered.

$$G_{PV}(s) = \frac{K_{PV}}{(1 + sT_{PV})} = \frac{\Delta P_{PV}}{\Delta \phi} \tag{5}$$

$$G_{DEG}(s) = \frac{K_{DEG}}{(1 + sT_{DEG})} = \frac{\Delta P_{DEG}}{\Delta u} \tag{6}$$

$$G_{FC_k}(s) = \frac{K_{FC}}{(1 + sT_{FC})} = \frac{\Delta P_{FC}}{\Delta P_{AE}} \quad k = 1, 2 \tag{7}$$

$$G_{WTG_k}(s) = \frac{K_{WTG}}{(1 + sT_{WTG})} = \frac{\Delta P_{WTG}}{\Delta P_W} \quad k = 1, 2, 3 \tag{8}$$

The mathematical modeling of wind speed, solar irradiation are explained in the following section.

5.1.1 Wind speed modeling

The generated power of the wind turbine generator (P_{WTG}) is a function of wind speed V_w . Wind speed is the algebraic summation of base wind speed with noise component (Pan and Das 2016).

V_w can be represented by

$$V_w = V_{WB} + V_{WN} \tag{9}$$

The base component of the wind speed is a constant which is present throughout the wind turbine operation and for the present case it is taken as 7.5 m/s. It can be represented as

$$V_{WB} = 7.5\phi(t) - 3\phi(t - 200) + 10.5\phi(t - 250) \tag{10}$$

where, $\phi(t)$ is the Heaviside step function. The wind speed noise is given by

$$V_{WN} = 2\sigma^2 \sum_{i=1}^N \sqrt{S_V(\omega_i)} \Delta\omega \cos(\omega_i t + \phi_i) \tag{11}$$

where $\omega_i = (i - 1/2)\Delta\omega$ and $\varphi_i \approx U(0, 2\pi)$. $\Delta\omega$ is the change in frequency to estimate spectral density. σ^2 is the variance due to noise and set to 200. The spectral density function $S_v(\omega_i)$ is expressed as

$$S_v(\omega_i) = \frac{2K_N F^2 |\omega_i|}{\pi^2 \left[1 + \left(F\omega_i / \mu\pi \right)^2 \right]^{4/3}} \tag{12}$$

$N = 50$ and $\Delta\omega = 0.5$ rad/s are considered to get an operative modelling precision. $K_N (= 0.004)$, $\mu (= 7.5)$ and $F (= 2000)$ denotes the surface drag coefficient, the base wind speed and the turbulence scale respectively.

5.1.2 Wind turbine characteristics

The power coefficient of wind turbine C_p (Pan and Das 2016) is characterized by non-dimensional curves which is a function of blade pitch angle (β) and tip speed ratio (λ). λ is given by

$$\lambda = \frac{R_{blade} \omega_{blade}}{V_w} \tag{13}$$

where $R_{blade} (= 23.5$ m) and $\omega_{blade} (= 3.14$ rad per sec) are the radius of blade and rotational speed of blade respectively.

Considering $\beta = 0.1745$, C_p is given by

$$C_p = (0.44 - 0.0167\beta) \sin \left[\frac{\pi(\lambda - 3)}{15 - 0.3\beta} \right] - 0.0184(\lambda - 3)\beta \tag{14}$$

The wind turbine output (Pan and Das 2016) is given by

$$P_w = \frac{1}{2} \rho A_r C_p V_w^3 \tag{15}$$

where $A_r = 1735$ m² is the blade swept area and $\rho = 1.250$ kg/m³ is the density of air.

5.1.3 Characteristic of photovoltaic system output power

The PV system output power of (Pan and Das 2016) is given by

$$P_{pv} = \eta S \gamma [1 - 0.005(T + 25)] \tag{16}$$

where η is the efficiency of the PV cells ($\eta = 10\%$). S is area of the PV array ($S = 4084$ m²), γ is the solar radiation on the PV cells in kw/m² and T is the ambient temperature ($T = 250$ °C).

ϕ is given by

$$\phi = 0.5\varphi(t) - 0.33\varphi(t - 25) + 0.3\varphi(t - 75) - 0.3\varphi(t - 150) + \varphi_n(t) \tag{17}$$

$$\varphi_n(t) \approx U(-0.1, 0.1)$$

5.1.4 Modeling of aqua electrolyzer

The dynamics of the aqua electrolyzer is modeled in (Li et al. 2008). AE makes hydrogen which is required for the fuel cell by utilizing a portion of the generated power from solar and wind (Pan and Das 2016; Ray et al. 2011). AE uses a fraction i.e. $(1 - k_n)$ of the total power generated from PV and WTG for the production of Hydrogen which is fed to the two FCs to produce power.

$$G_{AE}(s) = \frac{K_{AE}}{(1 + sT_{AE})} \tag{18}$$

k_n is taken as 0.6 for the present study.

5.1.5 Modeling of energy storing system

Energy storing components effectively absorb/supply deficit/surplus energy from/to the hybrid power system within a fraction of period for a stable hybrid system (Pan and Das 2016; Ray et al. 2011).

FESS and BESS are the two storage system considered in the present study and is expressed as

$$G_{FESS}(s) = \frac{K_{FESS}}{(1 + sT_{FESS})} \tag{19}$$

$$G_{BESS}(s) = \frac{K_{BESS}}{(1 + sT_{BESS})} \tag{20}$$

Each energy storage element is provided with an upper and lower saturation limit along with rate constraint non-linearity to prevent the mechanical shock due to sudden frequency variation (Pan 2015). Their generation limits are $|P_{FESS}| < 0.9$, $|P_{BESS}| < 0.2$ and $0 < P_{DEG} < 0.45$.

5.1.6 Power system model

The power system model is formulated as

$$G_{sys}(s) = \frac{\Delta f}{\Delta P_e} = \frac{1}{Ms + D} \tag{21}$$

where D and M are equivalent damping constant and inertia constant of the hybrid power system. It is taken as 0.4 and 0.03 respectively for the present study.

5.2 Adaptive fuzzy PID (AFPID) control

A fuzzy logic controller has a predefined set of control rules, which depends on researcher's knowledge and experience (Fereidouni et al. 2015). The input/output linguistic variables of the membership functions (MFs) are generally pre-determined in FLC. The design of FLCs largely depends on

the choice of input/output scaling factors (SF) and selection of controller parameters. Tuning of SFs is of highest importance because of their universal effect on the control action.

For satisfactory control action, the membership functions should be a function of error ‘e’ and change of error ‘Δe’ and FLC maps input to output by a limited number of IF-THEN rules. Sometimes this is not adequate to provide necessary control actions. In such cases, static values of SFs and single MFs are insufficient to achieve the desired control action. To overcome this, various online and offline methods are proposed to fine-tune the input/output SFs to change the definition of MFs.

Adaptive control has been a topic of research for various LFC schemes. Adaptive control technique is basically categorized into two types, the self-tuning regulators and the model reference control systems (Woo et al. 2000). Adaptive controller makes the system under control less sensitive to its parameter uncertainties under various environmental and operating conditions. Adaptive fuzzy based PID controller design has now been considered as a topic of research and several methods are adopted in (Savran and Kahraman 2014) and (Fereidouni et al. 2015). In the proposed method an adaptive PID kind FLC (AFPID) is used to get the process optimally controlled based on the ‘e’ and ‘Δe’. Figure 3 represents the schematic diagram of the proposed AFPID controller. The membership functions ‘e’ and ‘Δe’ are shown in Fig. 4 and rule base is depicted in Table 6. Both the fuzzy part 1 and fuzzy part 2 share a common membership function. This makes the design simple. The MFs for ‘e’ and ‘Δe’ are kept within the common interval [− 1, 1] and they are chosen to be triangular which is the most popular and economical as compared to other alternatives. Mamdani fuzzy interface is used for the present simulation. In Table 6, the fuzzy linguistic variables NB, NS, Z, PS, PB represents Negative Big, Negative Small, Zero, Positive Small and Positive Big respectively. The ISCA optimization algorithm is used for fine tuning of the input and output scaling factors (K1 to K2) and two cascade PID controller parameters (KP1, KI1, KD1, KP2, KI2, KD2) of AFPID controller shown in Fig. 3.

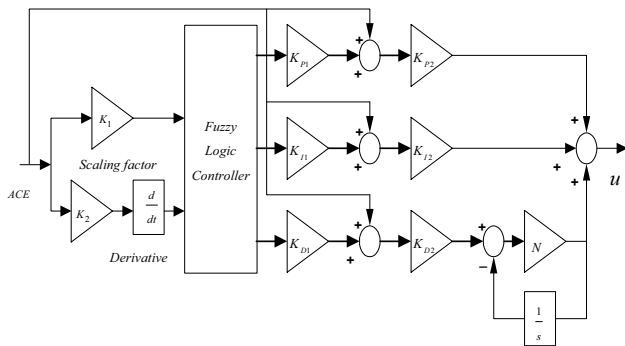


Fig. 3 Structure of the proposed adaptive fuzzy logic control scheme

ISE has taken into consideration in the present study for tuning of the controller gains.

$$J = \int_0^{T_{max}} [(\Delta f)^2 + (\Delta u)^2 / K_f] dt \tag{22}$$

where T_{max} is the maximum simulation time and Δf and Δu are the per unit frequency deviation and control signal output of controller. T_{max} is taken as 300 s for the present case. The factor K_f is chosen as 104 to give equal weightage on both parts of control objective.

5.3 Results and discussions

The autonomous power generating system is simulated by considering two different controllers i.e. PID and AFPID controller separately and optimized with the ISCA technique. Figure 5 depicts the stochastic output characteristics of the solar photovoltaic power (P_{PV}), wind turbine generator (P_{WTG}), the total power generated by the renewable sources (wind and PV) to the electric grid (P_T) and the load demand (P_L) which is used in the simulation study. Both the solar and wind power output have overlying variations about their steady state, which would of course affect the system frequency. These oscillations have to be damped out as quickly as possible by the proper control action of the controller. In the present design framework, both the powers (P_{WTG} and P_{PV}) drop to significantly different level after 25 s and 200 s respectively. This resembles the practical scenario as the generated powers of wind turbine and PV

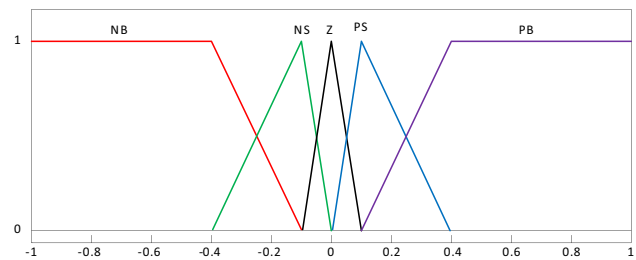


Fig. 4 Membership functions for e and Δe

Table 6 Rule base for AFPID

e	Δe				
	NB	NS	Z	PS	PB
NB	NB	NB	NS	NS	Z
NS	NB	NS	NS	Z	PS
Z	NS	NS	Z	PS	PS
PS	NS	Z	PS	PS	PB
PB	Z	PS	PS	PB	PB

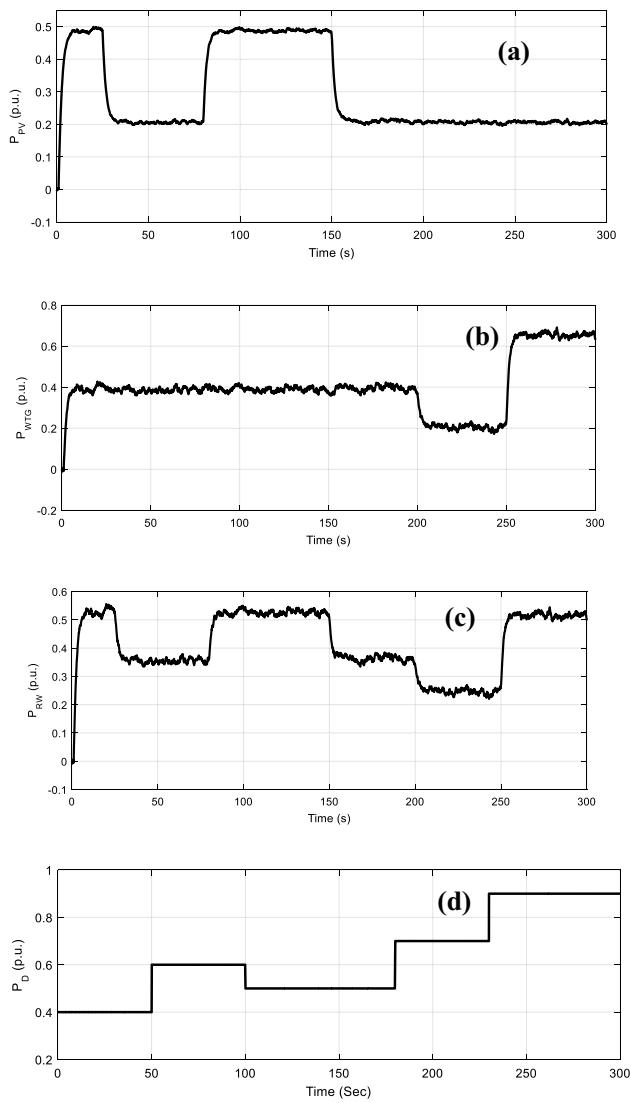


Fig. 5 Generated power by renewable sources and load demand which are independent of the controller structure **a** solar power, **b** wind power, **c** total renewable power and **d** load demand

system fluctuate widely over time based on the varied environmental conditions.

Simultaneously the load demand also faces an identical kind of variation about its steady state and varies from 0.9 to 0.4 p.u.. In addition, a time delay of 10 ms is considered for the controller input and output. The AFPID controller takes all these speculative variations into consideration while computing the controller gains. AFPID controller surpasses the PID controller results in minimum frequency deviation (Δf). A comparison is done with the conventional PID controller and corresponding analogous parameter for the PID and the AFPID controller are noted in Table 7. The corresponding values of objective function (J_{min}) is given in Table 7. Figure 6 illustrates the frequency and control signal deviation for the mWOA optimized AFPID and PID

Table 7 Improved SCA based tuning parameters of PID and AFPID controller

Controller	Optimized parameters	Objective function value
PID	KP=4.4577, KI=4.3060, KD=0.0335	8.3606
AFPID	K1=0.6384, K2=0.0245, KP1=4.6621, KI1=2.8857, KD1=3.8302, KP2=1.9728, KI2=3.6359, KD2=3.3998	3.6060

controller. It can be seen from Fig. 6a that, proposed AFPID controller structure provides better system dynamic response compared to conventional PID control structure. From the control characteristic as shown in Fig. 7b, it can be noticed that the band of oscillations for the AFPID controller is not as much as that of classical PID controller. From practical point of view this is relevant as the control signal activates mechanical components like DEG, BESS, FESS, etc. Prolonged swinging in the actuator demand would deteriorate the mechanical parts which degrade their life time as well as affect the performance of these components. The equivalent powers generated by the FC, BESS, FESS and DEG are given in Fig. 7. With the AFPID controller, the power fluctuation in these energy storage systems reduces significantly than that of conventional PID controller. This may result in smaller dimension of these energy storage and supply

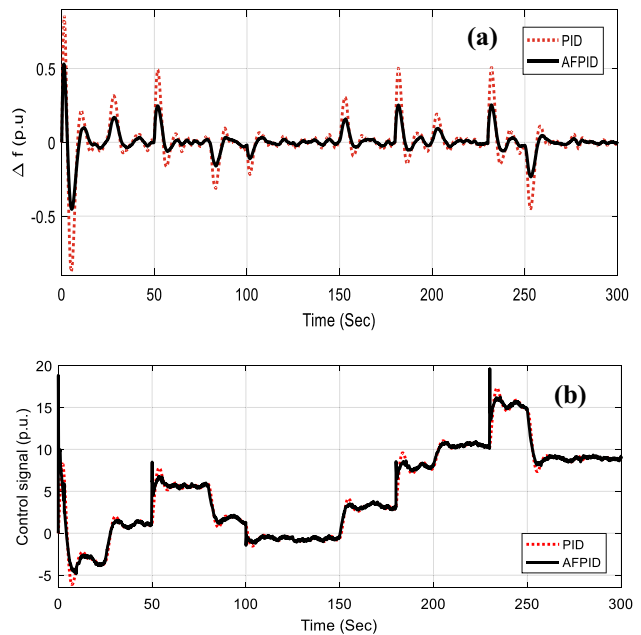


Fig. 6 **a** Frequency deviation and **b** control signal with PID and AFPID controller

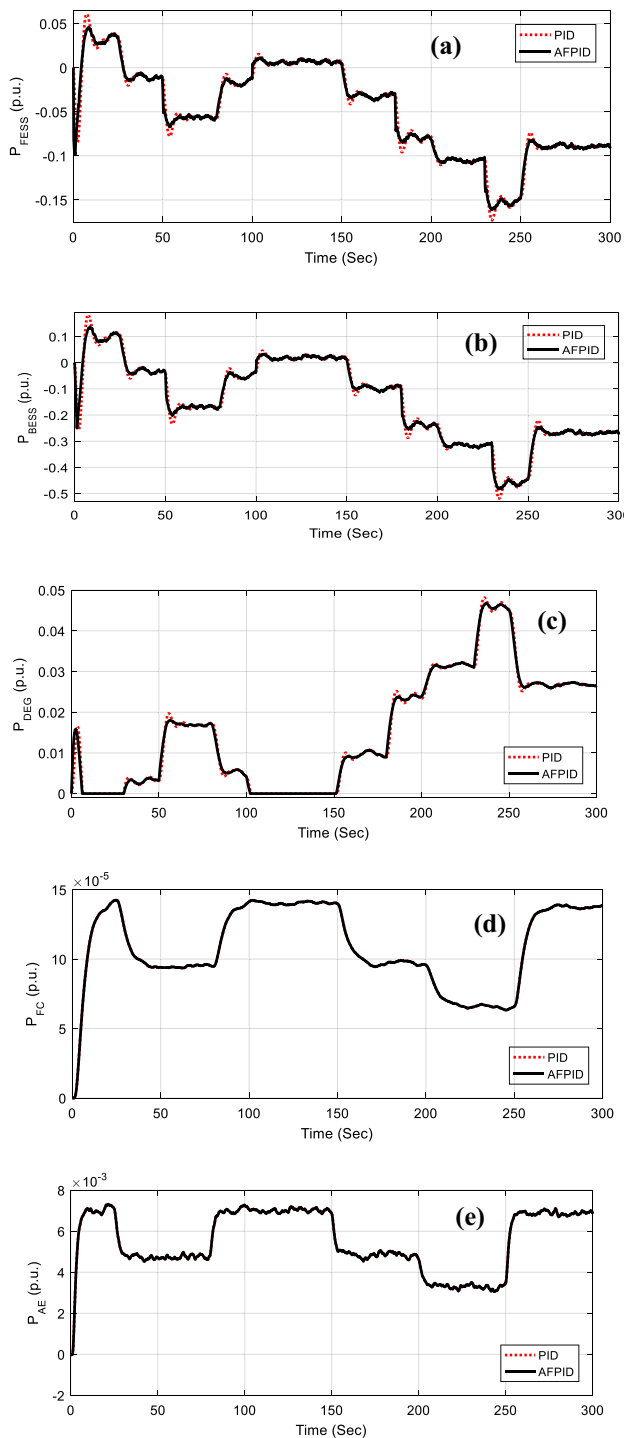


Fig. 7 Powers of various sources of autonomous power system with PID and AFPID controller. **a** Flywheel energy storage system, **b** battery energy storage system, **c** diesel energy generator, **d** fuel cell, and **e** aqua electrolyzer

systems. There is also less requirement of storing and supplying power to suppress the grid frequency variation.

Thus the hybrid power system becomes more reliable and energy efficient. In Fig. 7 negative powers in energy storage elements indicated that they are power absorbing and conversely the positive powers signify that they are producing the extra power making the whole system stable.

5.4 Sensitivity analysis and stability proof

5.4.1 Sensitivity analysis

The adaptive property of AFPID controller is also examined by sensitivity analysis by introducing variations in different hybrid power system parameters. This helps to evaluate the robustness of the proposed control approach with dynamical changes of power system parameters during abnormal operation or due to various environmental factors. Table 8 summarizes the objective function (J) value with increase/decrease of various parameter values like M , D , K_{FESS} , T_{FESS} , K_{BESS} and T_{BESS} for both ISCA optimized PID and AFPID controller. The change in J value have stated in Table 8 are calculated as: $\% \text{ change} = (J_{\text{nominal}} - J) \times 100 / J_{\text{nominal}}$. The positive $\%$ change in J value in Table 8 indicates decrease in J value (improvement in system performance) and negative $\%$ changes indicates increase in J value (deterioration in system performance). Analysis of results presented in Table 8 demonstrates that, the system behaviour is more or less the same as the percentage changes are less for all the cases as shown in Table 8. It is also obvious from Table 8 that with AFPID, the performance deterioration is less than that with the PID controller. As an example, the frequency deviation with 50% increase and decrease in M parameter with ISCA optimized PID and AFPID controller are shown in Figs. 8 and 9 respectively. This validates the adaptive nature of proposed ISCA optimized AFPID controller for frequency regulation in studied system with significant variations in the system parameters.

5.4.2 Stability proof

One of the requirement in any control system is that the control loop must be characterized by a sufficient degree of stability. Various criteria have been developed to prove stability or instability of a control system and Eigen value analysis is one of them. The system Eigen values with ISA optimized PID and AFPID controller are provided in Table 9. It is obvious from Table 9 that the eigenvalues lie in the left half of s -plane for both designed controller. Hence it can be concluded that the system is stable with ISCA optimized PID and AFPID controllers.

Table 8 Percentage change in objective function value (J) for system parameter variation

System Parameter	Perturbation	PID		AFPID	
		J value	% change	J value	% change
D	Increase 50%	7.8053	6.6419	3.5122	2.6012
	Decrease 50%	9.0148	-7.8248	3.7079	-2.8258
M	Increase 50%	8.2473	1.3552	3.4342	4.7643
	Decrease 50%	9.1671	-9.6464	4.1115	-14.0183
KDEG	Increase 50%	8.1874	2.0716	3.4490	4.3539
	Decrease 50%	8.5492	-2.2558	3.7769	-4.7393
TDEG	Increase 50%	8.4512	-1.0837	3.6479	-1.162
	Decrease 50%	8.1604	2.3946	3.5338	2.0022
KFESS	Increase 50%	6.7871	18.8204	2.8318	21.4698
	Decrease 50%	10.5605	-26.3127	4.7751	-32.421
TFESS	Increase 50%	8.4583	-1.1686	3.6316	-0.7099
	Decrease 50%	8.2678	1.1100	3.5852	0.5768
KBESS	Increase 50%	4.8039	42.5412	2.2575	37.396
	Decrease 50%	19.0054	-127.321	7.8571	-117.8896
TBESS	Increase 50%	8.6618	-3.6026	3.6156	-0.2662
	Decrease 50%	8.0892	3.2462	3.5979	0.2246
Time delay	Increase 50%	8.4391	-0.9389	3.615	-0.2496
	Decrease 50%	8.2841	0.9150	3.6001	0.1636

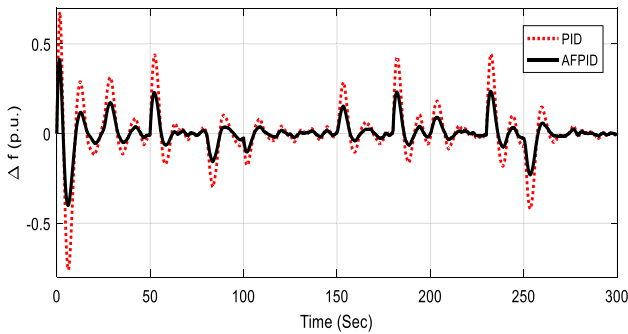


Fig. 8 Frequency deviation with 50% increase in M with PID and AFPID controller

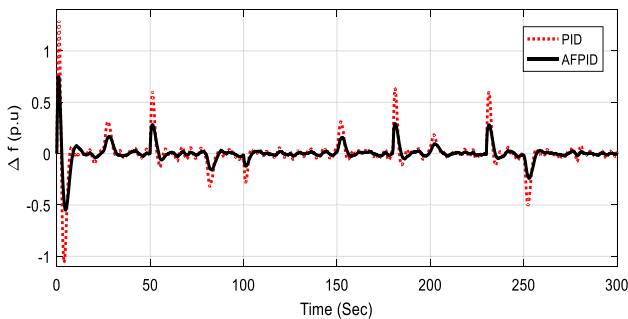


Fig. 9 Frequency deviation with 50% decrease in M with PID and AFPID controller

Table 9 System Eigen values with ISCA optimized PID and AFPID controller

With PID controller	With AFPID controller
-1.0	-1.0
-9.5783	-96.0336
-0.5171	-13.7094
-0.2398 + 0.6402i	-0.5115
-0.2398 - 0.6402i	-0.1603 + 0.3630i
-10.0	-0.1603 - 0.3630i
-0.25	-10.0
-0.25	-0.25
-2.0	-0.25
-0.5556	-2.00
-0.6667	-0.5556
-0.6667	-0.6667
-0.6667	-0.6667
	-0.6667

6 Conclusion

In practice, classical PID controller is commonly used for LFC problem. However, it is not able to provide desirable performance during severe disturbances. Owing to the practical difficulties faced in trying to achieve desired control criteria in LFC, an adaptive fuzzy logic control method is presented in this paper to control the frequency

deviation of the hybrid power system. For tuning the controller parameters, an improved SCA technique is proposed where the position of search agents are updated by using correction factors. Proposed algorithm is first applied to the benchmark unimodal and multimodal test functions designed to test the exploration and exploitation capability of an algorithm. It is found from the statistical results that the proposed ISCA algorithm outperform original SCA, PSO, GSA, and GWO algorithms. In the next stage, the frequency control of an autonomous power generating system consisting of various energy sources like DEG, FC, with renewable energy sources like PV units, WTG along with energy storage devices like BESS, FESS etc. and cluster of loads is considered and the parameters of proposed AFPID controller are optimized employing ISCA technique. It is observed that ISCA tuned AFPID controller provides superior performance compared to PID controller. The sensitivity analysis is also conducted on the proposed AFPID controller by introducing different hybrid power system parameters and the robustness of the proposed control approach with the dynamic change of power system parameters is evaluated. Finally, the stability of the proposed control system is tested using Eigen value analysis and the stability of the system is proved.

References

- Amin G, Shekari T, Sun A (2018) An adaptive optimization-based load shedding scheme in microgrids. In: Proceedings of the 51st Hawaii international conference on system sciences (HICSS). <https://doi.org/10.24251/HICSS.2018.337>
- Aminifar F, Shekari T (2018) An adaptive wide-area load shedding scheme incorporating power system real-time limitations. *IEEE Syst J* 12(1):1–9. <https://doi.org/10.1109/JSYST.2016.2535170>
- Bevrani H, Habibi F, Babahajyani P, Watanabe M, Mitani Y (2012) Intelligent frequency control in an AC microgrid: online pso-based fuzzy tuning approach. *IEEE Trans Smart Grid* 3(4):1935–1944. <https://doi.org/10.1109/TSG.2012.2196806>
- Bevrani H, Feizi MR, Ataee S (2015) Robust frequency control in an islanded microgrid H_{∞} and μ -synthesis approaches. *IEEE Trans Smart Grid* 7(2):706–717. <https://doi.org/10.1109/TSG.2015.2446984>
- Demars J (2006) Statistical comparisons of classifiers over multiple data sets. *J Mach Learn Res* 7:1–30
- Fereidouni A, Masoum MA, Moghbel M (2015) A new adaptive configuration of PID type fuzzy logic controller. *ISA Trans* 56:222–240. <https://doi.org/10.1016/j.isatra.2014.11.010>. <https://doi.org/10.2478/v10187-010-0029-0>
- Khooban MH, Niknam T, Blaabjerg F, Dragicevic T (2017) A new load frequency control strategy for micro-grids with considering electrical vehicles. *Electr Power Syst Res* 143:585–598. <https://doi.org/10.1016/j.epsr.2016.10.057>
- Lee DJ, Wang L (2008) Small-signal stability analysis of an autonomous hybrid renewable energy power generation/energy storage system part I: time-domain simulations. *IEEE Trans Energy Convers* 23(1):311–320. <https://doi.org/10.1109/TEC.2007.914309>
- Li X, Song YJ, Han SB (2008) Frequency control in micro-grid power system combined with electrolyzer system and fuzzy PI controller. *J Power Sources* 180(1):468–475. <https://doi.org/10.1016/j.jpowsour.2008.01.092>
- Mohanty SR, Kishor N, Ray PK (2014) Robust H-infinite loop shaping controller based on hybrid PSO and harmonic search for frequency regulation in hybrid distributed generation system. *Int J Electr Power Energy Syst* 60:302–316. <https://doi.org/10.1016/j.ijepes.2014.03.012>
- Nandar CSA (2013) Robust PI control of smart controllable load for frequency stabilization of microgrid power system. *Renew Energy* 56:16–23. <https://doi.org/10.1016/j.renene.2012.10.032>
- Pan I (2015) Kriging based surrogate modeling for fractional order control of microgrids. *IEEE Trans Smart Grid* 6(1):36–44. <https://doi.org/10.1109/TSG.2014.2336771>
- Pan I (2016) Fractional order fuzzy control of hybrid power system with renewable generation using chaotic PSO. *ISA Trans* 62:19–29. <https://doi.org/10.1016/j.isatra.2015.03.003>
- Pan I, Das S (2015) Fractional-order load-frequency control of interconnected power systems using chaotic multi-objective optimization. *Appl Soft Comput* 29:328–344. <https://doi.org/10.1016/j.asoc.2014.12.032>
- Pan I, Das S (2016) Fractional order AGC for distributed energy resources using robust optimization. *IEEE Trans Smart Grid* 7(5):2175–2186. <https://doi.org/10.1109/TSG.2015.2459766>
- Pandey SK, Mohanty SR, Kishor N, Catalao JPS (2014) Frequency regulation in hybrid power systems using particle swarm optimization and linear matrix inequalities based robust controller design. *Int J Electr Power Energy Syst* 63:887–900. <https://doi.org/10.1016/j.ijepes.2014.06.062>
- Pukar M, Chen Z, Bak-Jensen B (2010) Under frequency load shedding for an islanded distribution system with distributed generators. *IEEE Trans Power Deliv* 25(2):911–918. <https://doi.org/10.1109/TPWRD.2009.2032327>
- Rajesh KS, Dash SS, Rajagopal R (2017a) Hybrid improved firefly-pattern search optimised fuzzy aided PID controller for automatic generation control of power systems with multi-type generations. *Swarm Evolut Comput*. <https://doi.org/10.1016/j.swevo.2018.03.005>
- Rajesh KS, Dash SS, Rajagopal R, Sridhar R (2017b) A review on control of ac microgrid. *Renew Sustain Energy Rev* 71:814–819. <https://doi.org/10.1016/j.rser.2016.12.106>
- Ray PK, Mohanty SR, Kishor N (2010) Small-signal analysis of autonomous hybrid distributed generation systems in presence of ultracapacitor and tie-line operation. *J Electr Eng* 61(4):205–214
- Ray PK, Mohanty SR, Kishor N (2011) Proportional–integral controller based small-signal analysis of hybrid distributed generation systems. *Energy Convers Manag* 52(4):1943–1954. <https://doi.org/10.1016/j.enconman.2010.11.011>
- Savran A, Kahraman G (2014) A fuzzy model based adaptive PID controller design for nonlinear and uncertain processes. *ISA Trans* 53(2):280–288. <https://doi.org/10.1016/j.isatra.2013.09.020>
- Senjyu T, Nakaji T, Uezato K, Funabashi T (2005) A hybrid power system with using alternative energy facilities in isolated island. *IEEE Trans Energy Convers* 20(2):406–414. <https://doi.org/10.1109/TEC.2004.837275>
- Seyedali M (2016) SCA: a sine cosine algorithm for solving optimization problems. *Knowl Based Syst* 96:20–133. <https://doi.org/10.1016/j.knsys.2015.12.022>
- Seyedali M, Mirjalili SM, Lewis A (2014) Grey wolf optimizer. *Adv Eng Softw* 69:46–61. <https://doi.org/10.1016/j.advengsoft.2013.12.007>
- Singh VP, Mohanty SR, Kishor N, Ray PK (2013) Robust H-infinity load frequency control in hybrid distributed generation system. *Int J Electr Power Energy Syst* 46:294–305. <https://doi.org/10.1016/j.ijepes.2012.10.015>
- Sudha KR, Santhi RV (2011) Robust decentralized load frequency control of interconnected power system with generation rate

- constraint using type-2 fuzzy approach. *Int J Electr Power Energy Syst* 33:699–707. <https://doi.org/10.1016/j.ijepes.2010.12.027>
- Tohit S, Aminifar F, Sanaye Pasand M (2016) An analytical adaptive load shedding scheme against severe combinational disturbances. *IEEE Trans Power Syst* 31(5):4135–4143. <https://doi.org/10.1109/TPWRS.2015.2503563>
- Vachirasricirikul S, Ngamroo I (2012) Robust controller design of microturbine and electrolyzer for frequency stabilization in a microgrid system with plug-in hybrid electric vehicles. *Int J Electr Power Energy Syst* 43(1):804–881. <https://doi.org/10.1016/j.ijepes.2012.06.029>
- Vachirasricirikul S, Ngamroo I (2014) Robust LFC in a smart grid with wind power penetration by coordinated V2G control and frequency controller. *IEEE Trans Smart Grid* 5(1):371–380. <https://doi.org/10.1109/TSG.2013.2264921>
- Woo ZW, Chung HY, Lin JJ (2000) A PID type fuzzy controller with self-tuning scaling factors. *Fuzzy Sets Syst* 115(2):321–326. [https://doi.org/10.1016/S0165-0114\(98\)00159-6](https://doi.org/10.1016/S0165-0114(98)00159-6)

Publisher's Note Springer Nature remains neutral with regard to jurisdictional claims in published maps and institutional affiliations.